Histol Histopathol (2019) 34: 359-372

http://www.hh.um.es

Histology and Histopathology

From Cell Biology to Tissue Engineering

Changes in spatio-temporal localization of tripeptidyl peptidase II (TPPII) in murine colon adenocarcinoma cells during aggresome formation: a microscopy study based on a novel fluorescent proteasome inhibitor

L.P. Bialy[1], U. Kuckelkorn[2], P. Henklein[2], J. Fayet[3], G.M. Wilczyński[4], A. Kamiński[5] and I. Mlynarczuk-Bialy[1]

[1]Department of Histology and Embryology, Center for Biostructure Research, Medical University of Warsaw, Warszawa, Poland, [2]Institut für Biochemie, Charité - Universitätsmedizin Berlin, Berlin, Germany, [3]Department of Ophthalmology, First Medical Faculty, Medical University of Warsaw, [4]Laboratory of Molecular and Systemic Neuromorphology, Department of Neurophysiology, Nencki Institute of Experimental Biology PAS Warsaw and [5]Department of Transplantology and Central Tissue Bank, Center for Biostructure Research, Medical University of Warsaw, Warszawa, Poland

Summary. Extralysosomal proteolysis is a multistep process involving the Ubiquitin- Proteasome System (UPS) and supplementary peptidases. Tripeptidyl peptidase II (TPPII) is the most extensively characterized enzyme, supplementing and sometimes substituting for proteasomal functions. In response to proteasome inhibition, polyubiquitinated proteins acting as proteasome substrates aggregate with proteasomes and form aggresomes. Several proteasome inhibitors are used as anti-cancer drugs.

Thus, in our study, we used a novel fluorescent-tagged proteasome inhibitor BSc2118 to induce aggresome formation in C26 murine colon adenocarcinoma cells. It allowed us to obtain effective, inhibitor-based, proteasome staining *in vivo*. This method has been validated by standard post-fixed indirect immunostaining and also allowed co-immunodetection of TPPII and polyubiquitinated proteins under laser scanning confocal microscopy.

We found that in the absence of the inhibitor, TPPII is diffusely dispersed within the cytoplasm of C26 cells. The proteasome and ubiquitin-rich perinuclear region failed to display enhanced TPPII staining. However, when proteasome function was impaired by the inhibitor, TPPII associated more closely with both the proteasome and polyubiquitinated proteins via TPPII recruitment to the perinuclear region and subsequently into emerging aggresomal structures. Furthermore, we have demonstrated the dynamic recruitment of TPPII into the developing aggresome: TPPII in the early aggresome was dispersed within the central part but subsequently aggregated on the surface of this structure. In the mature aggresome of C26 cells TPPII formed a spherical mantle, which surrounded the round core containing proteasomes and polyubiquitinated proteins.

Our morphological data indicate that TPPII displays spatial localization with proteasomes especially upon proteasome inhibition in aggresomes of C26 cells.

Key words: TPPII, Proteasome, Ubiquitin, Aggresome, Proteasome inhibitor BSc2118

Offprint requests to: Izabela Mlynarczuk-Bialy MD, PhD, Department of Histology and Embryology, Center for Biostructure Research, Medical University of Warsaw, Chałubińskiego 5, 02-004 Warszawa, Poland. e-mal: izamlynar@esculap.pl or imlynarczuk@wum.edu.pl

DOI:10.14670/HH-18-042

Introduction

Tripeptidyl peptidase II (TPPII) participates in the extra-lysosomal protein degradation pathway downstream from the Ubiquitin- Proteasome System (UPS) (Mlynarczuk-Bialy, 2008; Rockel et al., 2012). The UPS degrades the majority of intracellular proteins in an ATP-dependent pathway (Hershko et al., 2000; Ciechanover, 2005). The substrates for the 26S proteasome undergo ATP-dependent polyubiquitination, a multistep process catalyzed by a cascade of E1, E2 and E3 enzymes (Hershko et al., 2000). However, the 20S core proteasome displays the ability to degrade unfolded

polypeptide chains without prior polyubiquitination (Ciechanover, 2005). The 26S proteasome is a 2.5-MDa multisubunit catalytic complex with three main proteolytic activities: trypsin-like, chymotrypsin-like and caspase-like attributed to the β1, β2 and β5 subunits respectively. They are located within the 20S catalytic core, with two 19S proteasome regulatory complexes forming the 26S proteasome (Voges et al., 1999). Degradation of unfolded polypeptide chains takes place inside the barrel-shaped catalytic chamber of the 20S core (Kruger et al., 2003).

Proteasome dependent proteolysis is a major pathway for generating MHC class I epitopes, which are short peptides derived from cellular proteins (Kloetzel, 2004). During the inflammatory process, predominantly due to interferon gamma (IFNγ) stimulation, three catalytic subunits of the 20S proteasome are replaced by the immunosubunits: β1i, β2i and β5i, forming the immunoproteasome, which features faster and more efficient antigen processing (Seifert et al., 2010).

Inhibition of the proteasome leads to accumulation of misfolded proteins and UPS components in the form of aggregates, which can be observed within the cell as single round, electron-dense protein-rich structures termed aggresomes (Wojcik et al., 1996; Wojcik, 1997; Johnston et al., 1998). The aggresome initially assembles in the peri-centriolar region of the cell by accumulation of polyubiquitinated proteins and proteasome complexes in a microtubule dependent manner (Wojcik et al., 1996; Wojcik, 1997). Subsequently other key cellular proteins are recruited into the aggresome (Sontag et al., 2017) including autophagy regulators p62 (Liu et al., 2016) and the cell cycle regulator CDK1 (Galindo-Moreno et al., 2017). The multifocal type of aggregates of polyubiquitinated proteins may also be observed in cells under specific conditions resulting from insufficient proteasome action to increased substrate generation e.g. by IFNγ stimulation (Seifert et al., 2010). These multifocal structures are termed aggresome-like structures - ALIS, and were first described as DALIS in dendritic cells during their maturation (Lelouard et al., 2002; Szeto et al., 2006).

Once formed, aggresomes cannot be removed by the UPS. Both aggresomes and ALIS have been shown to be substrates for autophagy (Wojcik et al., 1996; Szeto et al., 2006; Wong and Cuervo, 2010; Dikic, 2017). Moreover, proteasome inhibition can induce autophagy in cancer cells (Zhu et al., 2010). This type of autophagy is referred to as aggrephagy (Lamark and Johansen, 2012). However, autophagy is not the universal mechanism for clearance of aggresomes (Wong et al., 2008).

Proteasome inhibitors induce proteotoxic conditions by unfolded protein stress that can lead to cell death and they were shown to be effective against various cancer cell types in preclinical studies (Nowis et al., 2007; Szokalska et al., 2009). However, in clinical practice they have proven effective only in the treatment of multiple myeloma and mantle cell lymphoma (Teicher and Tomaszewski, 2015; Manasanch and Orlowski, 2017). Furthermore, disruption of aggresomes increases the anticancer activity of proteasome inhibitors (Nawrocki et al., 2006; Paoluzzi et al., 2009).

Following the release of the first proteasome inhibitor approved for human therapy, bortezomib, the evaluation of this proteasome inhibitor and several new inhibitors for their therapeutic potential is ongoing. One such example of a newly developed proteasome inhibitor is BSc2118 which is a derivative of the proteasome inhibitor MG132 (Braun et al., 2005). BSc2118 inhibits efficiently the 20S proteasome, thus promoting the accumulation of polyubiquitinated proteins in aggresomes, inducing apoptosis, cell cycle arrest at G2/M, and preventing NF-kappaB activation (Braun et al., 2005; Mlynarczuk-Bialy et al., 2006). Moreover, BSc2118 displays anti-myeloma and local anti-melanoma activity in animal models (Sterz et al., 2010; Mlynarczuk-Bialy et al., 2014; Zang et al., 2015).

Tripeptidyl peptidase II (TPPII) cooperates with the proteasome in sequential protein degradation. Recently, TPPII was found in close proximity with proteasomes in neurons (Fukuda et al., 2017). TPPII is a giant, self-compartmentalizing, twisted double stranded cytosolic peptidase complex of 6MDa, composed of stacked doublets of hemispherical dimers (Rockel et al., 2005). It displays both exo- and endo-proteolytic activities. The exoproteolytic activity of TPP II is localized within the active catalytic chamber of two stacked dimers. It can supplement the downstream action of the proteasome in sequential protein degradation through N-terminal trimming of tripeptides from oligopeptides released by the proteasome (Tomkinson and Lindas, 2005; Peters et al., 2011). In addition, TPPII can attack and degrade peptides longer than 15 amino acids (up to 75 AA) and unfolded substrates via its endoproteolytic activity (Eklund et al., 2012; Rockel et al., 2012), giving TPPII the ability to work not only downstream but also in parallel to the proteasome. Remarkably, TPPII expression is upregulated under proteasome inhibition, and it has been observed to substitute several functions of the inhibited proteasome (Glas et al., 1998; Geier et al., 1999). TPPII is also involved in generation of proteasome-independent MHC class I epitopes, thereby replacing proteasome in this process, especially when proteasome function is impaired (Seifert et al., 2003; Guil et al., 2006). Moreover, involvement of TPPII has been noted in many other important cellular processes: cell division, viability and apoptosis, regulation of MAP kinase pathways, antigen processing, as well as in muscle wasting and obesity (Rockel et al., 2012; Wiemhoefer et al., 2015; Mlynarczuk-Bialy, 2008). Importantly, the TPPII inhibitor AAF-cmk sensitized leukemic cells to pro-apoptotic cytokine action (Mlnarczuk et al., 2004) and TPPII is overexpressed in squamous cell carcinoma cells (Usukura et al., 2013). Therefore, TPPII is a valuable potential target for anticancer therapy (Mlnarczuk et al., 2004; Huai et al., 2008; Duensing et al., 2010).

Based on the presented evidence, we have hypothesized that TPPII may co-localize with elements of the UPS within aggresomes. Our main goal was to

analyze TPPII localization in murine adenocarcinoma C26 cells upon proteasomal inhibition while paying particular attention to the forming aggresomal structures. Our additional aim was to validate the use of novel red fluorescent-tagged BSc2118 proteasome inhibitor for direct vital staining of proteasome. To achieve these two aims, we combined vital inhibitor based staining of proteasome with classical post-fixed indirect immunocytochemical detection of TPPII and poly-ubiquitinated proteins in murine colon adenocarcinoma C26 cells using a laser scanning confocal microscopy (LSCM) approach.

Materials and methods

Cell culture

C26 murine colon adenocarcinoma cells (ATCC) were cultured in RPMI-1640 medium with stable glutamine (Biochrom, Germany) supplemented with 10% heat-inactivated FCS (Biochrom, Germany), 1% Antibiotic-Antimycotic (Thermo Fisher/Life Technologies, US) in 75 cm^2 tissue flasks (Greiner, Germany) and kept at 37°C in a 5% CO_2 humidified incubator.

Proteasome inhibitor synthesis

BSc2118 was synthesized as described in (Braun et al., 2005; Mlynarczuk-Bialy et al., 2014). Briefly, the peptide was synthesized by Fmoc strategy on an ABI-Peptide-Synthesizer 433A. As solid support preloaded H-L-Leucinol-2-Cl-Trt resin (1 g, loading 0.45 mmol/g) from CBL was used. The cleavage of the peptide from resin was performed with methylene chloride, 20% acetic acid 1% Trifluoroethanol, 10% Hexafluoro-2-propanol 2 times for 10 minutes on ice. Purification of the crude peptide was carried out using preparative HPLC under standard conditions (acetonitrile, water, trifluoro acetic acid). The correct mass was determined by MALDI mass spectrometry on a Voyager-DEPRO workstation.

The red fluorescent variant of BSc2118 was synthesized as follows: a solution of 0.01mmol of the peptide NH_2-Leu- Asp(tBu)-Leu-CHO (BSc2118) in 0.5 ml dimethylformamide DMF (pH=8.5) was added to 0.01 mmol of Bodipy-581/591 SE (Molecular Probes, Germany). The reaction mixture was stirred overnight in darkness and then purified by HPLC. The synthesized fluorescent inhibitor was dissolved in DMSO to obtain a 1mg/ml stock solution of BSc2118. In this article the red fluorescent BSc2118 variant is named as BSc2118-Traced Red (BSc2118-TR).

MEK inhibitor

Commercially available U0126 (Sigma, US) was dissolved in DSMO to the recommended stock concentration and added to the cultured cells in a final concentration of 5 μM.

CVDE (Crystal Violet Dye Elution) viability assay

10^4 cells per well were seeded in 96-well plates (Greiner, Germany) and incubated with fluorescent BSc2118-TR or U0126 or vehicle for 30 min or 24h. CVDE viability assay was performed as described in (Mlynarczuk-Bialy et al., 2006, 2014). Absorbance was measured at 570 nm using FLUOstar Omega (BMG LABTECH, Germany).

Measurement of proteasome activity within cells

10^6 cells/well in 96-well plates (Greiner, Germany) were incubated with BSc2118-TR or U0126 for 30min or 24h. Proteasome activity was measured in cell lysates using fluorescent substrate (Suc-LLVY-AMC, Bachem) as described in (Braun et al., 2005; Mlynarczuk-Bialy et al., 2014). Excitation 390 nm and emission 460 nm filters were used in FLUOstar Omega (BMG LABTECH, Germany).

Western blot

Cell lysates were assayed by a standard WB procedure as described elsewhere (Seifert et al., 2010). Briefly, cells were incubated with 0.5 μM or 5 μM BSc2118-TR or DMSO solvent for 24h. Lysates prepared in hypotonic buffer (20 mM TRIS-HCl, pH 7.5, 10 mM EDTA, 100 mM NaCl) with 1% NP40, containing proteinase inhibitors Complete® (Roche, France) supplemented with proteasome inhibitor-10 μM MG-132 (Calbiochem, USA) and inhibitor of deubiquitinylating enzymes-10 mM NEM (Sigma, USA). Subsequently, samples (containing 15 μg of protein in Laemmli sample buffer) underwent SDS-PAGE (12.5%) with semi-dry transfer onto nitrocellulose membrane, which was probed with appropriate primary antibody: FK2 (Enzo Biochem, US) or GAPDH (Santa Cruz, US) and horse radish conjugated secondary antibody (all from Santa Cruz). The signal was visualized by the ECL-chemiluminescence method using BioMax films (Kodak).

Cytochemistry procedures

Cell culture and fixation

For all cytochemical procedures cells were cultured onto multi-chamber slides (Becton Dickinson, US) and fixed using the modified routine procedure for cytopathology with ice-cold buffered 70% ethanol (pH 7.5; phosphate buffer) for 3 minutes and directly rehydrated (pH 7.5; phosphate buffer).

Antibodies and immunocytochemistry

The following antibodies were used for indirect immunofluorescence staining: goat polyclonal anti-TPPII antibody (Santa Cruz, US) at dilution 1:1000, mouse monoclonal FK2 antibody (Enzo Biochem, US)

recognizing selectively polyubiquitinated proteins at dilution 1:10 000, rabbit polyclonal anti 20S antibody at dilution 1:100 (Enzo Biochem, US). The secondary antibodies were anti-Fc affinity-purified Fab specific to goat, mouse or rabbit IgG conjugated with DyLight 488 or DyLight 680 (Jackson ImmunoResearch, US). The secondary antibodies were used at 1:10 000 dilution.

Nonspecific antibody binding was blocked for 60min in 10% BSA at RT. Incubation with primary antibodies in 3% BSA solution was performed overnight at 4°C, furthermore secondary antibodies were incubated for 1h in 37°C in a humidified atmosphere. Both prior to and after the secondary antibody incubation, slides were triple washed in phosphate-buffered saline (pH 7.4) with 0.1% Tween 20 (Sigma, US) for 10 minutes.

Fluorescent proteasome inhibitor BSc2118 for vital staining

The synthesized inhibitor was dissolved in DMSO to obtain 1 mg/ml stock solution of BSc2118. The final concentration of the inhibitor used during our experiments ranged from 0.5 μM to 5 μM. Detailed concentration for each experiment is given in the Experimental Procedures section. All required controls were treated with appropriate mock (DMSO) concentrations prior to fixation.

Experimental procedures

Basic proteasome staining protocol

C26 cells were stained by addition of BSc2118-TR to the culture media for 3 min at the final concentration of 5 μM. Subsequently cells were fixed (as described above), rehydrated and underwent classic post-fixed immunostaining for either 20S proteasome or polyubiquitinated proteins and TPPII.

Aggresome formation assay

C26 cells were incubated with 0.5-2.5 μM BSc2118-TR from 1.5 to 16 hours to induce aggresome formation (Table 1).

The steps in aggresome formation assay is as follows: DMSO (necessary for control) - then/or incubation with BSc2118-TR - followed by fixation/rehydratation - finally immunostaining.

The controls were incubated with DMSO solvent prior to fixation in the corresponding concentration and for at least the same time as aggresome formation groups as follows: Fig. 1C-24 h; Fig. 2A-16 h; Fig. 3A-6 h.

Embedding and laser scanning confocal microscopy

After cytochemical procedures, slides were embedded in Vecta Shield containing 4',6-diamidino-2-phenylindole (DAPI) (Vector Laboratories, US). The analysis and images were made using a confocal laser SP5 microscope equipped with appropriate lasers (HeNe 633 nm, DPSS diode 561 nm, and Argon laser: line 488 nm) and Las-AF software (Leica, Germany). Special care was applied to exclude cross-talk effects, and the images were scanned sequentially.

Results

BSc2118-TR does not affect C26 cell viability, efficiently inhibits proteasome activity and enables specific direct staining of proteasomes - validation of the cytochemical procedure

The viability of C26 cells was not significantly reduced by BSc2118-TR in both concentrations used in this study even after 24 h of incubation with the inhibitor. In contrast, the positive control agent MEK inhibitor U0126 (5 μM) reduced C26 cells viability to 50% after 24h of treatment with no effect after 30 min (Fig. 1A-two left panels).

BSc2118-TR in both studied concentrations (0.5 μM and 5 μM) effectively inhibited Suc-LLVY-AMC-hydrolyzing proteasome activity in cells following 30 min. incubation. Proteasome activity was still inhibited after 24 h (Fig. 1A-two right panels). The inhibition of proteasome-dependent proteolysis by BSc2118-TR after 24 h was also confirmed by Western Blot (Fig. 1B). BSc2118-TR in both studied concentrations (0.5 μM and 5 μM) resulted in accumulation of polyubiquitinated proteins.

The validation of the staining procedure is shown in Fig. 1C,D. As demonstrated in Fig. 1C, the vital inhibitor-based staining procedure of proteasomes (BSc2118-TR 3 min, 5 μM, prior to fixation) combined with subsequent ethanol based fixation enables efficient proteasome staining that is comparable to classic indirect immunocytochemical antibody based visualization. Using this procedure the signal of BSc2118-TR (Fig. 1C-red) was co-localized with 20S proteasome immunostained with polyclonal antibody (Fig. 1C-green). Moreover, this vital staining does not

Table 1. Detailed time-points of aggresome formation assay.

Time Point	0	1.5h	3h	5h	12-16h
BSc2118-TR Concentration	5 μM	2.5 μM	2.5 μM	2.5 μM	0.5 μM
BSc2118-TR Staining Time	3 min	1.5 h	3 h	5 h	12-16 h
Figure	1C; 2A; 3A	3B	3C	3D	1D; 2B; 4ABC

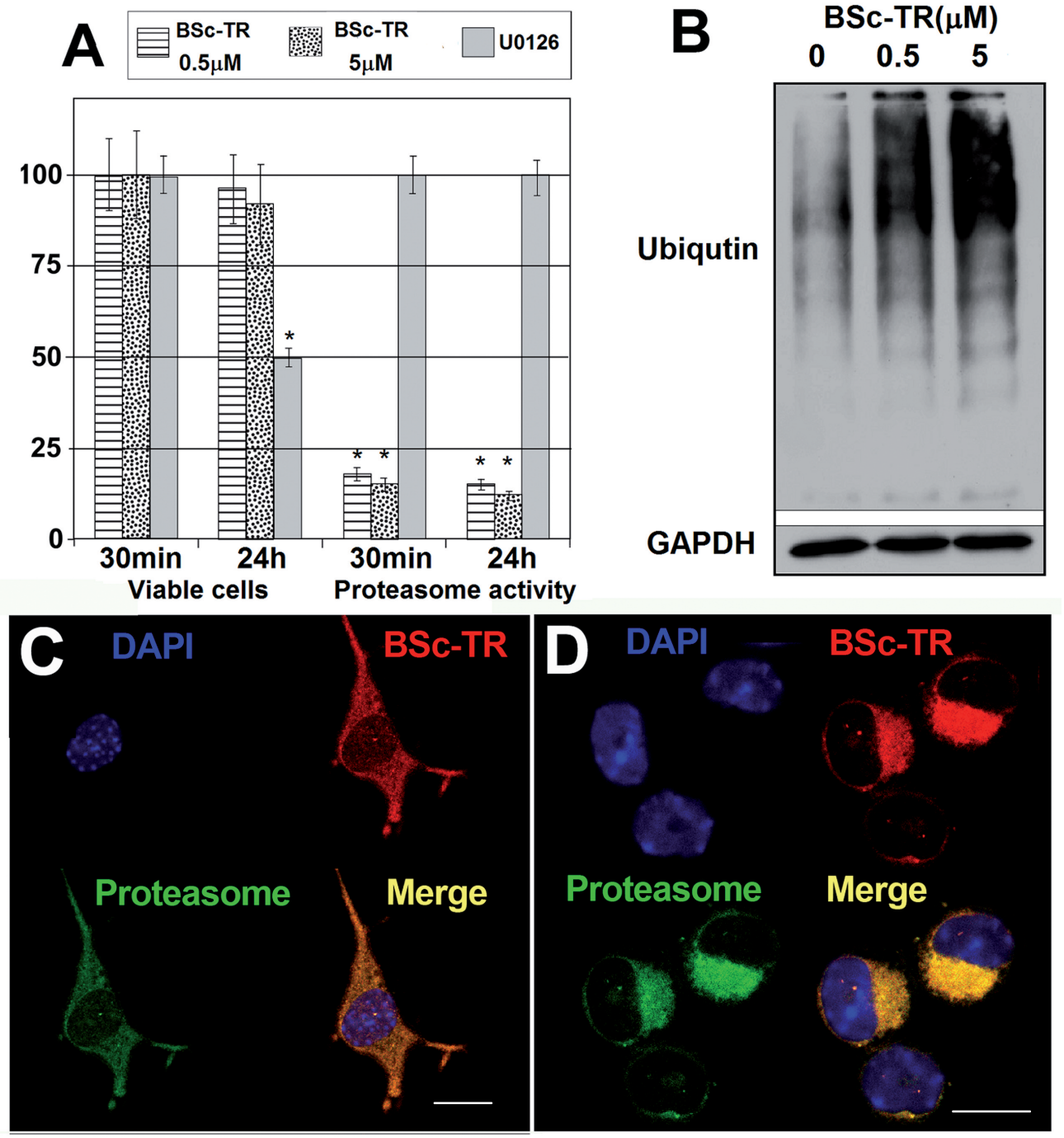

Fig. 1. Proteasome inhibition and detection by BSc2118-TR - Validation of the staining procedure. **A.** Viability of murine colon adenocarcinoma C26 cells measured by CVDE examination and proteasome Suc-LLVY-AMC-hydrolyzing activity in cell lysates. Cell viability after 30min and 24h incubation with BSc2118-TR (0.5 μM and 5 μM) is not significantly affected whereas proteasome activity is efficiently reduced in both concentrations. MEK inhibitor - U0126 (5μM) reduces cell viability to 50% after 24h and does not affect proteasome activity. Bars represent SEM. *$p<0.05$, (t-Student test). **B.** Accumulation of polyubiquitinated proteins in Western Blot. After 24h BSc2118-TR induces accumulation of polyubiquitinylated proteins (lanes 2 and 3) in comparison to the solvent treated cells (lane 1). GAPDH- a loading control. **C, D.** Comparison of cytochemical vital staining of proteasome with BSc2118-TR (red) to classic indirect immunocytochemical 20S proteasome antibody-based staining (green); nuclei (blue) and merged. **C.** Basic vital proteasome staining: The BSc2118-TR (5 μM) staining for 3 min prior to fixation. **D.** Aggresome Formation Assay: BSc2118-TR (0.5 μM) incubation for 24h prior to fixation. The fluorescent inhibitor-based proteasome signal co-localizes both within the cytoplasm as well as within the nucleus with antibody immunolabeling. There is no cytopathic or aggregative effect of proteasome inhibitor using the vital staining protocol combined with alcohol based fixation **(C)**, while prolonged proteasome inhibition induces cytopathic changes including aggresome formation **(D)**. Cells in vital basic proteasome staining protocol **(C)** were incubated with DMSO solvent (in the same concentration as in Aggresome Formation Assay - **D**) for 24h prior to proteasome staining and fixation to exclude DMSO effect on cell morphology during BSc2118-TR incubation for 24h. x 400.

affect cell morphology. We did not observe either cytopathic effect of proteasome inhibitor or solvent or any aggregative effect of inhibitor or fixative (Figs. 1C, 3B), while prolonged (24 h) proteasome inhibition by 0.5 μM BSc2118-TR resulted in changes of cell shape and induced formation of proteasome-rich aggresomes (Fig. 1D). Moreover, during aggresome formation, the BSc2118-TR signal (Fig. 1D-red) was also co-localized with 20S proteasome signal as immunostained with polyclonal antibody within aggresomes (Fig. 1D-green).

We therefore validated the use of direct inhibitor-based staining of proteasomes with subsequent ethanol based fixation without additional immunostaining of the proteasome in C26 cells in the later steps of this study.

TPPII is localized diffusely in the cytoplasm and not in the nuclei of C26 cells

In the control cells, TPPII immunoreactivity was observed within the cytoplasm whereas the nuclei remained repeatedly negative. Its cytoplasmic signal was strong, displaying a diffuse staining pattern which was rather homogenous and without any signs of perinuclear clustering or dotting (general view in Fig. 2A-green, detailed in Fig. 3A-green).

In contrast to TPPII, both proteasome and polyubiquitinated proteins demonstrated signal not only in the cytoplasm, but also within the nuclei, presenting as nuclear foci (Figs. 2A, 3A-red/magenta, Fig. 1D-green). Slightly stronger immunoreactivity of the proteasome and polyubiquitinated proteins was observed in the perinuclear region (Figs. 2A, 3A-red/magenta). At the same time a corresponding stronger signal of TPPII was absent from that region (Figs. 2A, 3A-geen). Moreover, in some cells, the TPPII signal appeared to be diminished in this region (Fig. 3A-green and merge). In contrast to that observation, both TPPII immuno-reactivity (Figs. 2B, 3C,D, 4A,B,C-green) as well as proteasome and polyubiquitinated protein immuno-

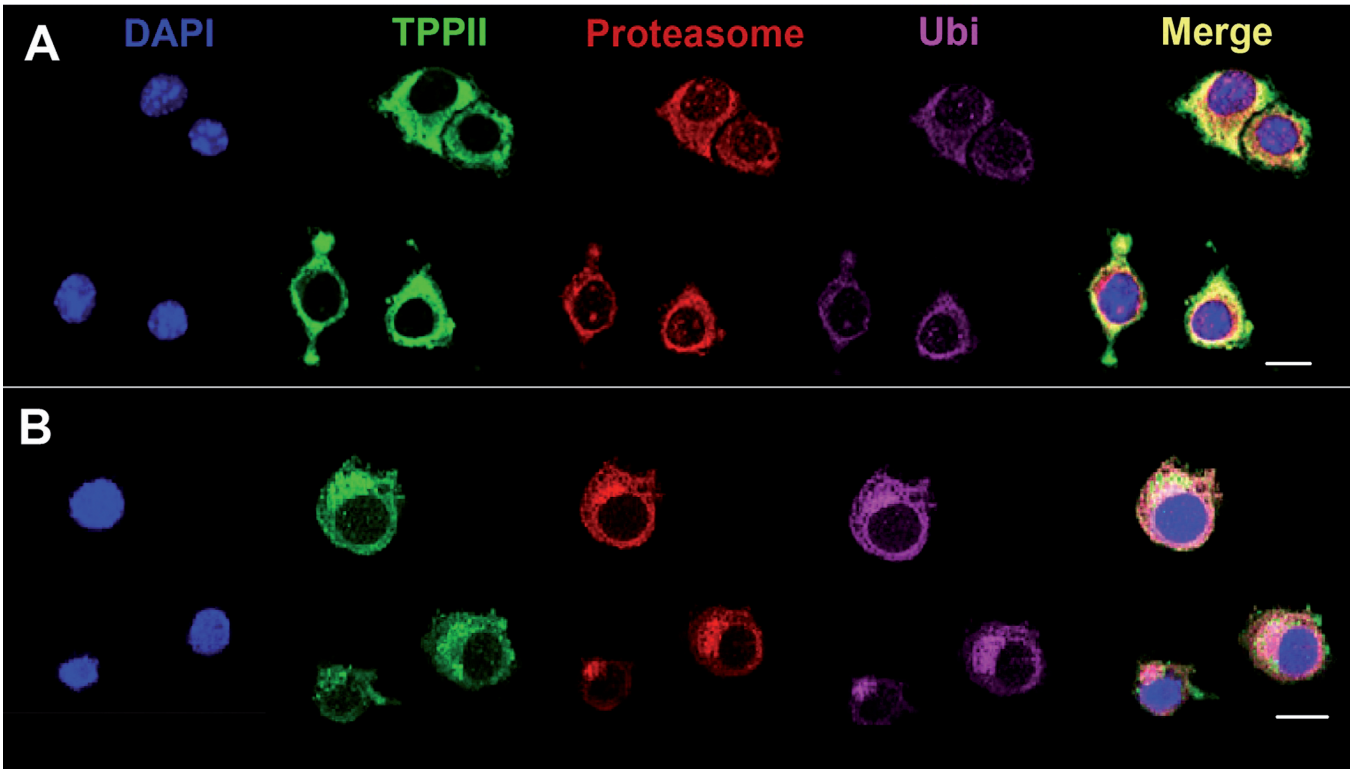

Fig. 2. General view of localization of TPPII and UPS in C26 cells **A.** The control C26 cells stained for TPPII (green), proteasome (red), polyubiquitinated proteins (magenta), nuclei (blue) and merged. Note a homogenous cytoplasmic green (TPPII) staining whereas red (proteasome) and magenta (polyubiquitinated proteins) signal predominates in the perinuclear region with signal also present within the nuclear foci. The magenta signal (polyubiquitinated proteins) in control cells is lower than in **B**. **B.** Late aggresome in C26 cells incubated with BSc2118-TR (0.5 μl/ml) for 16 h. nuclei (blue), TPPII (green), proteasome (red), polyubiquitinated proteins (magenta), and merged. Note the big single aggresome positive for red (proteasome) and magenta (polyubiquitinated proteins) signal that can be seen in the perinuclear region. In contrast to the control cells from panel **A**, the green (TPPII) staining is not homogenous, but it gives the maximal signal in the perinuclear area. The detailed structure of the mature aggresome is displayed in Fig. 4. Scale bars: 10 µm.

reactivity (Figs. 2B, 3C,D, 4A,B,C-red/magenta) was strongly enhanced in the perinuclear region under proteasome inhibition.

BSc2118-TR induces formation of a large aggresome in C26 cells

The proteasome inhibitor BSc2118-TR induced aggresome formation in a time and dose dependent manner. The mature aggresome in C26 cells appears as a single, large, circular structure (Fig. 2B, 4A) containing proteasomes (red) and polyubiquitinated proteins (magenta). It was primarily organized in the perinuclear region (Fig. 3B) and subsequently formed a larger structure occupying a substantial area of the cytoplasm (Fig. 2B, 4A red/magenta), occasionally modulating the shape of the nucleus of C26 cells (4A, 4B lower panel - blue). Analysis of multiple images revealed that 83%

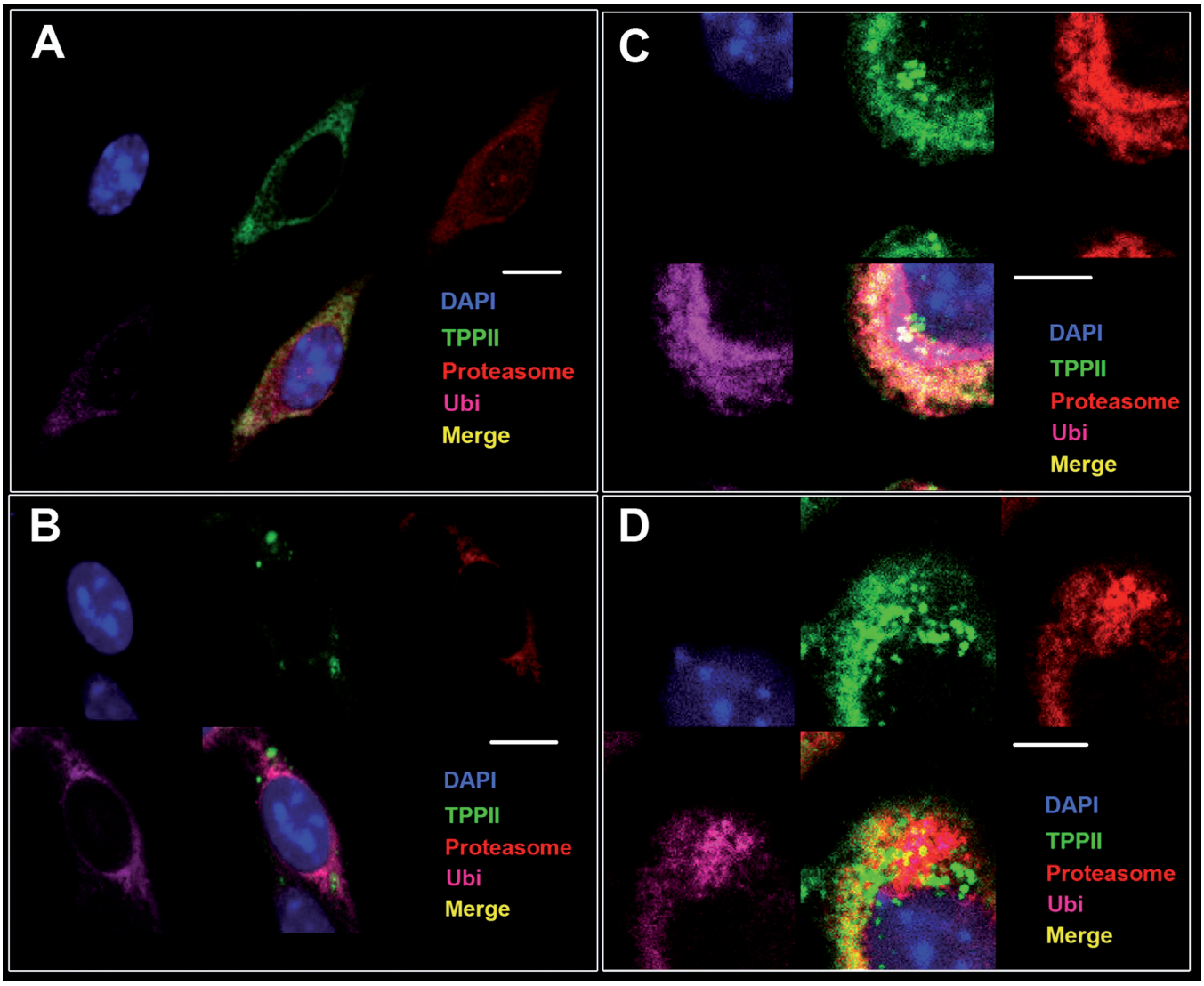

Fig. 3. Early aggresome. The subsequent stages of aggresome formation in C26 cells incubated with BSc2118-TR: nuclei (blue), TPPII (green), proteasome (red), polyubiquitinated proteins (magenta), and merged. **A.** The control C26 cells stained with BSc2118-TR for 3min. Note a slight magenta signal of polyubiquitinated proteins in the control cells. The green signal (TPPII) does not strictly co-localize with red (proteasome) and magenta(polyubiquitinated proteins) signals. **B.** C26 cells incubated with BSc2118-TR (2.5 μM) for 1.5h. Note the stronger magenta (polyubiquitinated proteins) and red (proteasome) signal and the green TPPII dots within the perinuclear region among them. **C.** C26 cells incubated with BSc2118-TR (2.5 μM) for 3h. The dot-like green (TPPII) signal is present in the central part of the forming aggresome surrounded by both red (proteasome) and magenta (polyubiquitinated proteins) staining. **D.** C26 cells incubated with BSc2118-TR(2.5 μM) for 6h. The dot-like green (TPPII) signal begins to surround the red (proteasome) and magenta (polyubiquitinated proteins) staining around the core of the aggresome. Scale bars: A, B, 10 µm; C, D, 5 µm.

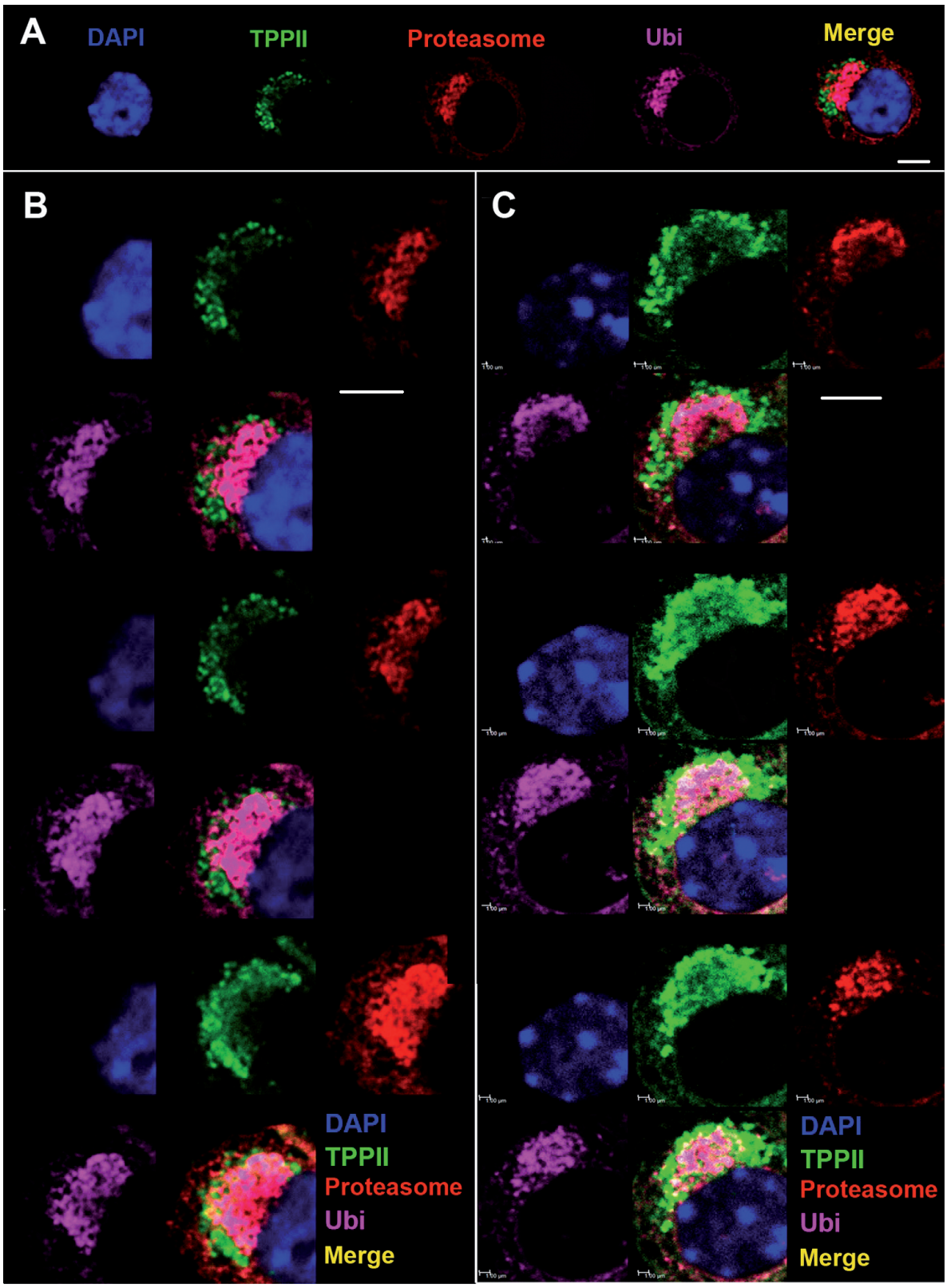

Fig. 4. Mature aggresome. C26 cells incubated with BSc2118-TR (0.5 μM) for 16h: nuclei (blue), TPPII (green), proteasome (red), polyubiquitinated proteins (magenta), and merged. **A.** Staining of the selected C26 cell. Note the dot-like green (TPPII) signal around the red (proteasome) and magenta (polyubiquitinated proteins) staining of the core of the aggresome. **B.** The detailed structure of the mature aggresome in the cell from panel A from serial confocal planes. Note the modulation of nucleus shape (blue) in middle and lower panel. **C.** The detailed structure of the mature aggresome in another selected C26 cell from serial confocal planes. **B, C.** Note that on the serial confocal plane sections, the dot-like green (TPPII) signal forming the spherical mantle surrounding the round core of the aggresome that is positive for both red (proteasome) and magenta (polyubiquitinated proteins) staining. **C** upper panel. Note the upper confocal plane with crescent-shaped red (proteasome) and magenta (polyubiquitinated proteins) aggregation surrounding the small "inner core" which is less positive for both red and magenta signal (proteasome and polyubiquitinated proteins) but with presence of low-abundant (two) green dots (TPPII). Scale bars: A, 10 µm; B, C, 5 µm.

(SD 4.5) of cells had big aggresomes, i.e. with diameters comparable to those of cell nuclei. Hence in other cells the aggresomal structures were smaller.

TPPII is recruited into the aggresome during early stages of its formation and forms a mantle in a mature aggresome of C26 cells

Initial signs of proteasome and polyubiquitinated protein aggregation within the perinuclear region were observed after 90 min of proteasome inhibition (Fig. 3B). The proteasome/polyubiquitinated proteins signal was remarkably stronger in the perinuclear region (Fig. 3B-red/magenta) in comparison to control cells (Fig. 3A), while the dot-like TPPII signal (Fig. 3B-green) was present in the center of the forming aggresome in close proximity to proteasomes and polyubiquitinated proteins within the perinuclear region and in the closely surrounding space.

During the ensuing steps of aggresome formation (Fig. 3C), TPPII displayed a strong dot-like staining pattern within the forming aggresome. Its dispersed signal was observed in aggresome center as TPPII containing foci (Fig. 3C-green) among poly-ubiquitinated proteins (magenta) and proteasomes (red). Together with the formation of dense proteasome and polyubiquitinated protein containing core (Fig. 3D-red/ magenta), the dot-like TPPII signal became more pronounced at the surface of the aggresome core (Fig. 3D-green).

Prolonged proteasome inhibition resulted in translocation of TPPII signal from the central area of the aggresome to the peripheral part of the mature aggresome (Fig. 4A-C-green). As is shown on the serial stacks of the mature aggresome (Fig. 4B,C), the signal for TPPII displayed a spherical mantle-like appearance around the round dense core of the aggresome. The aggresome core displayed strong immunoreactivity for both the proteasome (red) and polyubiquitinated proteins (magenta), but was only slightly positive for TPPII (green).

In C26 cells, the estimated maximal diameter of the whole mature aggresome with TPPII mantle reached approx. 11 μm. The diameter of the core was approx. 8.5 μm, and the diameter of the area within the core with predominantly proteasome/polyubiquitinated proteins signal was measured at approx. 5 μm. The estimated maximal diameter of the nucleus was approx. 14 μm (measured from several random plane sections through the middle part of the aggresome and nucleus-approximate estimation; SD 0.8; 0.8; 0.2; 0.5, respectively).

Furthermore, we were able to observe, in rare cases, and on several limited adjacent confocal planes, a small inner core, which was only slightly positive for proteasomes and polyubiquitinated proteins (Fig. 4C-upper and middle panel-red/magenta). Occasionally, in the middle part of this region, low-abundance dots of TPPII signal were visualized (Fig. 4C-green). Nevertheless, there was no corresponding increase of TPPII signal in this area.

Discussion

Staining of enzymes through binding of fluorescent inhibitors provides an alternative to classic immunolabeling for both microscopy and flow cytometry, with the advantage of reducing possible antibody cross-reactivity especially with multi-color staining (Marchetti et al., 2004; Darzynkiewicz et al., 2011). Inhibitor based detection of proteasomes in biosensors enables proteasome and immunoproteasome quantitative measurement in serum (Patent Pending PL: P.396170; P.396171; P.417435). Moreover, various fluorescent proteasome reporters are suitable for visualization of proteasome localization within living cells including aggresomes (Berkers et al., 2007).

Fluorochrome-tagged derivates of the novel proteasome inhibitor BSc2118 were designed by our research group for visualization of inhibitor distribution in organs and tissues after its parenteral administration in animal models (Doeppner et al., 2012; Mlynarczuk-Bialy et al., 2014). Previously, we have published and confirmed that vital proteasome staining in cells *in vitro* with green fluorescent BSc2118-FL is fully comparable with an indirect immunocytochemistry method (Mlynarczuk-Bialy et al., 2014).

In this manuscript, we provide data for the red fluorescent BSc2118 derivative. Furthermore, it was combined with intracellular localization of polyubiquitin staining using an FK2 antibody as an aggresome marker. Thus, our findings make a substantial contribution to cytochemical methods as we demonstrate a novel approach in which this direct vital pre-fixed inhibitor-based proteasome staining can be efficiently combined with post-fixed classic immunocytochemical detection of other cellular components.

The down side of any fluorescent-inhibitor technique is that high inhibitor concentrations are required for initial staining and such high concentration cannot be used for prolonged studies, as it leads to the inhibition of the target enzyme, which triggers severe physiological side effects (including cell death). Therefore, lower inhibitor concentrations must be used for longer time-points in kinetics studies.

A high inhibitor concentration is required for basic proteasome staining (BSc2118-TR 5 μM for 3 min). Conveniently, 0.5 μM BSc2118-TR was sufficient to stain proteasomes and induces aggresome formation after 24h without inducing cell death.

Extralysosomal proteolysis is a multistep process involving the action of UPS and downstream acting peptidases such as TPPII. The products released by 20/26S proteasomes are oligopeptides comprised of 4 to 25 AA (Voges et al., 1999; Kruger et al., 2003). In order for complete degradation, the action of additional peptidases is required. This can be achieved via TPPII, which can also digest substrates longer than 15 AA (Reits et al., 2004; York et al., 2006). TPPII was described as being involved in several processes of cell regulation (Mlynarczuk-Bialy, 2008; Rockel et al., 2012). At a cellular level, the response to impaired

UPS proteolysis is the formation of an aggresome containing UPS components (Wojcik and DeMartino, 2003).

In our study, we evaluated the recruitment of TPPII into the aggresomal structures as well as the cytoplasmic localization of TPPII in murine colon adenocarcinoma C26 cells. We investigated anticancer properties of various proteasome inhibitors against several cancer cell lines (Pleban et al., 2001; Mlynarczuk-Bialy et al., 2014). Among them C26 cells respond to proteasome inhibition by formation of giant aggresomes, while they can survive long-term proteasome inhibition (e.g. 1 μM MG-132 for 24 h) making them an ideal candidate for an aggresome formation study (unpublished data). However, C26 cells are sensitive to MEK kinase inhibitors, thus we used U0126 as a positive cytotoxicity control agent in CVDE assay.

Despite the low-abundance of TPPII in most cells and tissues (Rockel et al., 2012), we demonstrated strong TPPII immunoreactivity within the cytoplasm, which corresponds well with published biochemical data that TPPII is a cytosolic peptidase (Tomkinson and Lindas, 2005; Rockel et al., 2012). In spite of this evidence, TPPII was reported to be found within the nucleus of cells exposed to various DNA-damaging anticancer drugs or agents inducing reactive oxygen species (Preta et al., 2009, 2010). Since BSc2118, similar to other proteasome inhibitors, demonstrates anticancer activity (Braun et al., 2005; Mlynarczuk-Bialy et al., 2006, 2014; Sterz et al., 2010; Zang et al., 2015), one could also expect nuclear relocation of TPPII signal under BSc2118 action. Despite that, BSc2118 did not cause nuclear translocation of TPPII, thus creating the argument for its unique anticancer mechanism of action. However, one has to keep in mind a relative resistance of C26 cells to proteasome inhibitor BSc2118-TR. Furthermore, proteasome inhibitors are not DNA-damaging agents in contrast to those classic drugs used by Preta et al. (2009, 2010).

TPPII cooperates with proteasomes in degradation of proteins and it was shown to directly interact with some UPS substrates such as p53 and SIRT7 (Nahalkova, 2015). Therefore, one can expect similar cellular distribution of those two components. As discussed above, in contrast to UPS, we do not find any TPPII immunoreactivity within the nuclei of C26 cells, suggesting that in this compartment either downstream proteolysis is performed by other enzymes or peptides are transported to the cytoplasm for further degradation in this cell line.

As we have shown, TPPII co-localizes with proteasomes in the majority of the cytoplasm in cells with fully functional proteasomes (no proteasome inhibitor added). TPPII immunoreactivity was not enhanced in the perinuclear region. Nevertheless, based on the sequential protein degradation and increased proteasome staining, we hypothesized that TPPII should be preferentially localized to this region. The perinuclear ER-rich region is a primary "proteolytic center" for intensive breakdown of newly synthesized proteins from Defective Ribosomal Products (DRiPs) by proteasomes, and thereby a source of precursors of MHC class I epitopes (Schubert et al., 2000; Kloetzel, 2004; Seifert et al., 2010). However, the precise role of TPPII in the generation of MHC I epitopes is still not established (Rockel et al., 2012).

Our data presented in this manuscript promote the idea that fully functional ubiquitin-proteasome proteolysis can be sufficient for proper proteolysis in perinuclear region of C26 cells without the need for significant TPPII involvement in this process. This observation is congruent with data suggesting that TPPII is not required for generation of most MHC class I epitopes, although it is necessary for proper trimming of some longer precursors via exoproteolytic activity (York et al., 2006). In any case, TPPII houses many catalytic chambers, whereas each proteasome contains only a single catalytic chamber, thus, the smaller amount of TPPII within the perinuclear region can be sufficient for downstream trimming of substrates. Moreover, it was recently published that, in hippocampal neurons, the ratio of proteasomes to TPPII is approximately 20 to 1 and only 7% of proteasome particles reveal spatial association with TPPII (Fukuda et al., 2017). However, there is no available co-localization data within any cancer cells.

Our data indicate that when the function of proteasomes is impaired by an inhibitor, TPPII appears to be more closely associated with both the proteasome and polyubiquitinated proteins. This reinforces the idea that TPPII has the potential to partially support some proteasomal functions in protein degradation, given that proteasome proteolysis is impaired. It has previously been well documented that TPPII generates HIV epitope independently from the proteasome (Seifert et al., 2003) and is indispensable for viral antigen processing (Guil et al., 2006), as well as maintaining viral growth in host cells (Zhang et al., 2011) under proteasome inhibition. Moreover, apart from the proteasome, TPPII seems to be the only cellular peptidase which degrades peptides containing more than 15 amino acids (Reits et al., 2004; York et al., 2006). Consequently, there is no alternative cytosolic pathway for degradation of substrates longer than 15 amino acid residues upon proteasome inhibition.
The formation of protein aggregates under proteasome inhibition was first reported by Wojcik et al. in 1996, however, the term aggresome was coined later (Johnston et al., 1998). The term aggresome describes the single structure induced by proteasome inhibition, which contains both the accumulated polyubiquitinated proteins as well as proteasomes and is localized in the perinuclear region of the cell. Ubiquitinated proteins are transported along microtubules to the pericentriolar proteolytic center of the cell and under proteasome inhibition they are stored there as an aggresome (Wojcik et al., 1996). Subsequently other key cellular proteins are recruited into the aggresome (Hartl, 2017; Manasanch and Orlowski, 2017; Sontag et al., 2017).

The accumulation of misfolded proteins within the aggresome is a postulated mechanism of action of proteasome inhibitors as anticancer drugs. Moreover, aggresome disruption by histone deacetylase inhibitors (Nawrocki et al., 2006) and microtubule acting agents (Miyahara et al., 2016) can augment the anticancer activity of proteasome inhibitors.

One should keep in mind that apart from TPP II, autophagy can potentially compensate for impaired proteasome-dependent proteolysis (Lamark and Johansen, 2012; Dikic, 2017). However, this aggrephagy" it is not a universal pathway for clearance of aggresomes (Wong et al., 2008). Moreover, the classical autophagy adaptor p62 was shown to be involved in aggresome formation (Liu et al., 2016) and together with HDAC6 mediates recruitment of key cellular proteins into aggresome in response to proteasome inhibition i.e. CKD1 (Galindo-Moreno et al., 2017).

In this study we observe big aggregates of polyubiqitinated proteins in the majority of C26 cells (84%), but nevertheless they do not compromise cell vitality. However one should keep in mind that CVDE corresponds to the total cell number but not strictly with cell well-being. Furthermore in some C26 cells aggregates are smaller and it is possible that these aggregates can be successfully cleared by an autophagic pathway. However, the phenomenon of C26 cell resistance to proteasome inhibition needs further studies. In our paper we show for the first time that TPPII is recruited into the aggresome during its formation using the model of colon adenocarcinoma C26 cells. Recently published literature describing rat hippocampal neurons stated that the number of proteasome particles at a distance closer than 110nm from TPPII is above the random distribution. Thereby, it is suggested that TPPII and the proteasome display a spatial relationship with each other (Fukuda et al., 2017). This data was obtained within the cells with fully functional proteasomes, whereas we focused on examining adenocarcinoma cells under impaired proteasome proteolytic conditions by BSc2118. Nonetheless, the data obtained by us strongly supports those findings in a different cell model.

Furthermore, we additionally describe an unknown part of the aggresome in C26 adenocarcinoma cells- the mantle formed by TPPII. Specifically, we found that in C26 cells during initial proteasome inhibition (during early stages of aggresome formation) TPPII is surrounded by proteasomes. At early time points of proteasome inhibition, the TPPII dispersed signal was present in the center of the forming aggresome, which was close to the perinuclear region and among both proteasomes and polyubiquitinated proteins.

Based on our original observations, we propose a model of TPPII recruitment and relocation in the aggresome in murine colon adenocarcinoma C26 cells. Following proteasome inhibition, TPPII is recruited to the perinuclear region into the central component of an early forming aggresome conceivably to support or substitute the impaired proteasomal function in protein degradation and most likely due to its endoproteolytic activity. This is followed by further aggresome organization with more TPPII complexes that are engaged for protein degradation. As aggresome formation intensifies, TPPII accumulates at the surface of aggregate in the form of a spherical mantle which surrounds the round dense core containing proteasomes and polyubiquitinated proteins. Moreover, the transition zone can be distinguished at the border of the core and the mantle. This zone is occupied by both proteasomes and polyubiquitinated protein as well as TPPII. We also cannot exclude the existence of the inner core with residual low-abundance TPPII.

Therefore, in contrast to the early stages of aggresome formation in murine colon adenocarcinoma C26 cells, under prolonged proteasome inhibition, TPPII aggregates at the surface before finally forming its spherical mantle. Hence, in the mature aggresome in C26 cells, TPPII surrounds both proteasome and polyubiquitinated proteins. The proposed model of mature aggresome structure and formation in colon adenocarcinoma C26 cells is displayed in Fig. 5. However, one must keep in mind that the choice of the cell line is peculiar - it forms very big aggresomes, it is relatively resistant to proteasome inhibitor anticancer action and is an old aneuploid cell line barring genetic alterations which may affect TPPII expression and/or

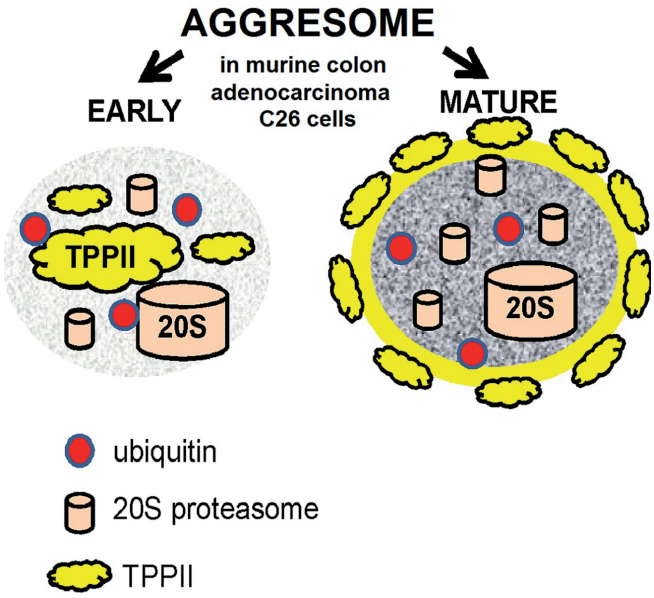

Fig. 5. Schematic presentation of aggresome changes during its maturation in murine colon adenocarcinoma C26 cells. In the early aggresome (left panel) TPPII starts to accumulate in the central region forming an aggresome complex with polyubiquitinated proteins and proteasome. In the mature aggresome (right panel): polyubiquitinated proteins with proteasome form a round dense core, shifting TPPII into the peripheral spherical mantle of the aggresome.

localization. Thus general functionality of this model may be limited.

Conclusion

In summary, we have confirmed our hypothesis that TPPII will be recruited to the aggresome formed by proteasome inhibition and the recruitment of TPPII into the aggresome in murine colon adenocarcinoma C26 cells is in accordance with published data suggesting that TPPII activity supplements and can even substitute impaired proteasomal function. However, the details of the involvement of TPPII in proteasome substitution and aggresome clearance will require a synthetic biochemical approach investigation in other cell lines as well.

Acknowledgments. We thank Prof. Dr. Peter-Michael Kloetzel (Charité - Universitätsmedizin Berlin) and Prof. Dr. Boris Schmidt (Technische Universität Darmstadt) for the generous gift of the novel proteasome inhibitor BSc2118, Dr. Cezary Wojcik (OHSU, Portland, OR) for his advice, reading and revision of the final version of the manuscript and Prof. Darek Gorecki (School of Pharmacy and Biomedical Sciences, University of Portsmouth, UK) for linguistic advice, and Mr. Maciej Krzywicki for excellent graphic assistance.

Financial support. The work was supported by financial resources of Medical University of Warsaw (1M15/WB2/10) to ŁB and by the European Regional Development Fund POIG 01.01.02-00-008/08, and by the grant from Polish National Center no. UMO-2013/08/M/NZ3/00655 (both to GW).

Conflict of interest. The authors declare no conflict of interest.

References

Berkers C.R., van Leeuwen F.W., Groothuis T.A., Peperzak V., van Tilburg E.W., Borst J., Neefjes J.J. and Ovaa H. (2007). Profiling proteasome activity in tissue with fluorescent probes. Mol. Pharm. 4, 739-748.

Braun H.A., Umbreen S., Groll M., Kuckelkorn U., Mlynarczuk I., Wigand M.E., Drung I., Kloetzel P.M. and Schmidt B. (2005). Tripeptide mimetics inhibit the 20 s proteasome by covalent bonding to the active threonines. J. Biol. Chem. 280, 28394-28401.

Ciechanover A. (2005). Proteolysis: From the lysosome to ubiquitin and the proteasome. Nat. Rev. Mol. Cell. Biol. 6, 79-87.

Darzynkiewicz Z., Pozarowski P., Lee B.W. and Johnson G.L. (2011). Fluorochrome-labeled inhibitors of caspases: Convenient *in vitro* and *in vivo* markers of apoptotic cells for cytometric analysis. Methods Mol. Biol. 682, 103-114.

Dikic I. (2017). Proteasomal and autophagic degradation systems. Annu. Rev. Biochem. 86, 193-224.

Doeppner T.R., Mlynarczuk-Bialy I., Kuckelkorn U., Kaltwasser B., Herz J., Hasan M.R., Hermann D.M. and Bahr M. (2012). The novel proteasome inhibitor BSc2118 protects against cerebral ischaemia through HIF1a accumulation and enhanced angioneurogenesis. Brain 135, 3282-3297.

Duensing S., Darr S., Cuevas R., Melquiot N., Brickner A.G., Duensing A. and Munger K. (2010). Tripeptidyl peptidase II is required for c-myc-induced centriole overduplication and a novel therapeutic target in c-myc-associated neoplasms. Genes Cancer 1, 883-892.

Eklund S., Dogan J., Jemth P., Kalbacher H. and Tomkinson B. (2012). Characterization of the endopeptidase activity of tripeptidyl-peptidase II. Biochem. Biophys. Res. Commun. 424, 503-507.

Fukuda Y., Beck F., Plitzko J.M. and Baumeister W. (2017). In situ structural studies of tripeptidyl peptidase II (TPPII) reveal spatial association with proteasomes. Proc. Natl. Acad. Sci. USA 114, 4412-4417.

Galindo-Moreno M., Giraldez S., Saez C., Japon M.A., Tortolero M. and Romero F. (2017). Both p62/sqstm1-hdac6-dependent autophagy and the aggresome pathway mediate cdk1 degradation in human breast cancer. Sci. Rep. 7, 10078.

Geier E., Pfeifer G., Wilm M., Lucchiari-Hartz M., Baumeister W., Eichmann K. and Niedermann G. (1999). A giant protease with potential to substitute for some functions of the proteasome. Science 283, 978-981.

Glas R., Bogyo M., McMaster J.S., Gaczynska M. and Ploegh H.L. (1998). A proteolytic system that compensates for loss of proteasome function. Nature 392, 618-622.

Guil S., Rodriguez-Castro M., Aguilar F., Villasevil E.M., Anton L.C. and Del Val M. (2006). Need for tripeptidyl-peptidase II in major histocompatibility complex class i viral antigen processing when proteasomes are detrimental. J. Biol. Chem. 281, 39925-39934.

Hartl F.U. (2017). Protein misfolding diseases. Annu. Rev. Biochem. 86, 21-26.

Hershko A., Ciechanover A. and Varshavsky A. (2000). Basic medical research award. The ubiquitin system. Nat. Med. 6, 1073-1081.

Huai J., Firat E., Nil A., Million D., Gaedicke S., Kanzler B., Freudenberg M., van Endert P., Kohler G., Pahl H.L., Aichele P., Eichmann K. and Niedermann G. (2008). Activation of cellular death programs associated with immunosenescence-like phenotype in TPPII knockout mice. Proc. Natl. Acad. Sci. USA 105, 5177-5182.

Johnston J.A., Ward C.L. and Kopito R.R. (1998). Aggresomes: A cellular response to misfolded proteins. J. Cell Biol. 143, 1883-1898.

Kloetzel P.M. (2004). The proteasome and MHC class I antigen processing. Biochim. Biophys. Acta 1695, 225-233.

Kruger E., Kuckelkorn U., Sijts A. and Kloetzel P.M. (2003). The components of the proteasome system and their role in mhc class i antigen processing. Rev. Physiol. Biochem. Pharmacol. 148, 81-104.

Lamark T. and Johansen T. (2012). Aggrephagy: Selective disposal of protein aggregates by macroautophagy. Int. J. Cell Biol. 2012, 736905.

Lelouard H., Gatti E., Cappello F., Gresser O., Camosseto V. and Pierre P. (2002). Transient aggregation of ubiquitinated proteins during dendritic cell maturation. Nature 417, 177-182.

Liu W.J., Ye L., Huang W.F., Guo L.J., Xu Z.G., Wu H.L., Yang C. and Liu H.F. (2016). P62 links the autophagy pathway and the ubiqutin-proteasome system upon ubiquitinated protein degradation. Cell. Mol. Biol. Lett. 21, 29.

Manasanch E.E. and Orlowski R.Z. (2017). Proteasome inhibitors in cancer therapy. Nat. Rev. Clin. Oncol. 14, 417-433.

Marchetti C., Gallego M.A., Defossez A., Formstecher P. and Marchetti P. (2004). Staining of human sperm with fluorochrome-labeled inhibitor of caspases to detect activated caspases: Correlation with apoptosis and sperm parameters. Hum. Reprod. 19, 1127-1134.

Miyahara K., Kazama H., Kokuba H., Komatsu S., Hirota A., Takemura J., Hirasawa K., Moriya S., Abe A., Hiramoto M., Ishikawa T. and

Miyazawa K. (2016). Targeting bortezomib-induced aggresome formation using vinorelbine enhances the cytotoxic effect along with er stress loading in breast cancer cell lines. Int. J. Oncol. 49, 1848-1858.

Mlnarczuk I., Mroz P., Hoser G., Nowis D., Bialy L.P., Ziemba H., Grzela T., Feleszko W., Malejczyk J., Wojcik C., Jakobisiak M. and Golab J. (2004). AAF-CMK sensitizes tumor cells to trail-mediated apoptosis. Leuk. Res. 28, 53-61.

Mlynarczuk-Bialy I. (2008). Enigmatic tripeptidylpeptidase II - protease for special tasks. Adv. Cell Biol. 35, 427-439.

Mlynarczuk-Bialy I., Roeckmann H., Kuckelkorn U., Schmidt B., Umbreen S., Golab J., Ludwig A., Montag C., Wiebusch L., Hagemeier C., Schadendorf D., Kloetzel P.M. and Seifert U. (2006). Combined effect of proteasome and calpain inhibition on cisplatin-resistant human melanoma cells. Cancer Res. 66, 7598-7605.

Mlynarczuk-Bialy I., Doeppner T.R., Golab J., Nowis D., Wilczynski G.M., Parobczak K., Wigand M.E., Hajdamowicz M., Bialy L.P., Aniolek O., Henklein P., Bahr M., Schmidt B., Kuckelkorn U. and Kloetzel P.M. (2014). Biodistribution and efficacy studies of the proteasome inhibitor BSc2118 in a mouse melanoma model. Transl. Oncol. 7, 570-579.

Nahalkova J. (2015). Novel protein-protein interactions of TPPII, p53, and sirt7. Mol. Cell. Biochem. 409, 13-22.

Nawrocki S.T., Carew J.S., Pino M.S., Highshaw R.A., Andtbacka R.H., Dunner K. Jr, Pal A., Bornmann W.G., Chiao P.J., Huang P., Xiong H., Abbruzzese J.L. and McConkey D.J. (2006). Aggresome disruption: A novel strategy to enhance bortezomib-induced apoptosis in pancreatic cancer cells. Cancer Res. 66, 3773-3781.

Nowis D., McConnell E.J., Dierlam L., Palamarchuk A., Lass A. and Wojcik C. (2007). TNF potentiates anticancer activity of bortezomib (velcade) through reduced expression of proteasome subunits and dysregulation of unfolded protein response. Int. J. Cancer 121, 431-441.

Paoluzzi L., Scotto L., Marchi E., Seshan V.E. and O'Connor O.A. (2009). The anti-histaminic cyproheptadine synergizes the antineoplastic activity of bortezomib in mantle cell lymphoma through its effects as a histone deacetylase inhibitor. Br. J. Haematol. 146, 656-659.

Peters J., Schonegge A.M., Rockel B. and Baumeister W. (2011). Molecular ruler of tripeptidylpeptidase II: Mechanistic principle of exopeptidase selectivity. Biochem. Biophys. Res. Commun. 414, 209-214.

Pleban E., Bury M., Mlynarczuk I. and Wojcik C. (2001). Effects of proteasome inhibitor PSI on neoplastic and non-transformed cell lines. Folia Histochem. Cytobiol. 39, 133-134.

Preta G., de Klark R. and Glas R. (2009). A role for nuclear translocation of tripeptidyl-peptidase II in reactive oxygen species-dependent DNA damage responses. Biochem. Biophys. Res. Commun. 389, 575-579.

Preta G., de Klark R., Chakraborti S. and Glas R. (2010). MAP kinase-signaling controls nuclear translocation of tripeptidyl-peptidase II in response to DNA damage and oxidative stress. Biochem. Biophys. Res. Commun. 399, 324-330.

Reits E., Neijssen J., Herberts C., Benckhuijsen W., Janssen L., Drijfhout J.W. and Neefjes J. (2004). A major role for TPPII in trimming proteasomal degradation products for MHC class I antigen presentation. Immunity 20, 495-506.

Rockel B., Peters J., Muller S.A., Seyit G., Ringler P., Hegerl R., Glaeser R.M. and Baumeister W. (2005). Molecular architecture and assembly mechanism of drosophila tripeptidyl peptidase II. Proc. Natl. Acad. Sci. USA 102, 10135-10140.

Rockel B., Kopec K.O., Lupas A.N. and Baumeister W. (2012). Structure and function of tripeptidyl peptidase II, a giant cytosolic protease. Biochim. Biophys. Acta 1824, 237-245.

Schubert U., Anton L.C., Gibbs J., Norbury C.C., Yewdell J.W. and Bennink J.R. (2000). Rapid degradation of a large fraction of newly synthesized proteins by proteasomes. Nature 404, 770-774.

Seifert U., Maranon C., Shmueli A., Desoutter J.F., Wesoloski L., Janek K., Henklein P., Diescher S., Andrieu M., de la Salle H., Weinschenk T., Schild H., Laderach D., Galy A., Haas G., Kloetzel P.M., Reiss Y. and Hosmalin A. (2003). An essential role for tripeptidyl peptidase in the generation of an mhc class i epitope. Nat. Immunol. 4, 375-379.

Seifert U., Bialy L.P., Ebstein F., Bech-Otschir D., Voigt A., Schroter F., Prozorovski T., Lange N., Steffen J., Rieger M., Kuckelkorn U., Aktas O., Kloetzel P.M. and Kruger E. (2010). Immunoproteasomes preserve protein homeostasis upon interferon-induced oxidative stress. Cell 142, 613-624.

Sontag E.M., Samant R.S. and Frydman J. (2017). Mechanisms and functions of spatial protein quality control. Annu. Rev. Biochem. 86, 97-122.

Sterz J., Jakob C., Kuckelkorn U., Heider U., Mieth M., Kleeberg L., Kaiser M., Kloetzel P.M., Sezer O. and von Metzler I. (2010). Bsc2118 is a novel proteasome inhibitor with activity against multiple myeloma. Eur. J. Haematol. 85, 99-107.

Szeto J., Kaniuk N.A., Canadien V., Nisman R., Mizushima N., Yoshimori T., Bazett-Jones D.P. and Brumell J.H. (2006). Alis are stress-induced protein storage compartments for substrates of the proteasome and autophagy. Autophagy 2, 189-199.

Szokalska A., Makowski M., Nowis D., Wilczynski G.M., Kujawa M., Wojcik C., Mlynarczuk-Bialy I., Salwa P., Bil J., Janowska S., Agostinis P., Verfaillie T., Bugajski M., Gietka J., Issat T., Glodkowska E., Mrowka P., Stoklosa T., Hamblin M.R., Mroz P., Jakobisiak M. and Golab J. (2009). Proteasome inhibition potentiates antitumor effects of photodynamic therapy in mice through induction of endoplasmic reticulum stress and unfolded protein response. Cancer Res. 69, 4235-4243.

Teicher B.A. and Tomaszewski J.E. (2015). Proteasome inhibitors. Biochem. Pharmacol. 96, 1-9.

Tomkinson B. and Lindas A.C. (2005). Tripeptidyl-peptidase II: A multi-purpose peptidase. Int. J. Biochem. Cell. Biol. 37, 1933-1937.

Usukura K., Kasamatsu A., Okamoto A., Kouzu Y., Higo M., Koike H., Sakamoto Y., Ogawara K., Shiiba M., Tanzawa H. and Uzawa K. (2013). Tripeptidyl peptidase II in human oral squamous cell carcinoma. J. Cancer. Res. Clin. Oncol. 139, 123-130.

Voges D., Zwickl P. and Baumeister W. (1999). The 26S proteasome: A molecular machine designed for controlled proteolysis. Annu. Rev. Biochem. 68, 1015-1068.

Wiemhoefer A., Stargardt A., van der Linden W.A., Renner M.C., van Kesteren R.E., Stap J., Raspe M.A., Tomkinson B., Kessels H.W., Ovaa H., Overkleeft H.S., Florea B. and Reits E.A. (2015). Tripeptidyl peptidase II mediates levels of nuclear phosphorylated ERK1 and ERK2. Mol. Cell. Proteomics 14, 2177-2193.

Wojcik C. (1997). An inhibitor of the chymotrypsin-like activity of the proteasome (PSI) induces similar morphological changes in various cell lines. Folia Histochem. Cytobiol. 35, 211-214.

Wojcik C. and DeMartino G.N. (2003). Intracellular localization of proteasomes. Int. J. Biochem. Cell Biol. 35, 579-589.

Wojcik C., Schroeter D., Wilk S., Lamprecht J. and Paweletz N. (1996).

Ubiquitin-mediated proteolysis centers in hela cells: Indication from studies of an inhibitor of the chymotrypsin-like activity of the proteasome. Eur. J. Cell Biol. 71, 311-318.

Wong E. and Cuervo A.M. (2010). Integration of clearance mechanisms: The proteasome and autophagy. Cold Spring Harb. Perspect. Biol 2, a006734.

Wong E.S., Tan J.M., Soong W.E., Hussein K., Nukina N., Dawson V.L., Dawson T.M., Cuervo A.M. and Lim K.L. (2008). Autophagy-mediated clearance of aggresomes is not a universal phenomenon. Hum. Mol. Genet. 17, 2570-2582.

York I.A., Bhutani N., Zendzian S., Goldberg A.L. and Rock K.L. (2006). Tripeptidyl peptidase II is the major peptidase needed to trim long antigenic precursors, but is not required for most MHC class I antigen presentation. J. Immunol. 177, 1434-1443.

Zang M., Li Z., Liu L., Li F., Li X., Dai Y., Li W., Kuckelkorn U., Doeppner T.R., Hermann D.M., Zhou W., Qiu L. and Jin F. (2015). Anti-tumor activity of the proteasome inhibitor BSc2118 against human multiple myeloma. Cancer Lett. 366, 173-181.

Zhang J., Wong J., Gao G. and Luo H. (2011). Tripeptidyl peptidase II serves as an alternative to impaired proteasome to maintain viral growth in the host cells. FEBS Lett. 585, 261-265.

Zhu K., Dunner K. Jr and McConkey D.J. (2010). Proteasome inhibitors activate autophagy as a cytoprotective response in human prostate cancer cells. Oncogene 29, 451-462.

Accepted September 18, 2018